

Thermal Effect on Pressure Distribution in Simulated High-Rise Buildings: Experiment and Analysis



K.H. Lee

T. Lee, Ph.D.

H. Tanaka, Ph.D.

ASHRAE Student Member

ABSTRACT

A study has been made, both experimentally and analytically, on the characteristics of thermal performance of high-rise buildings using an idealized model building with a number of openings at various locations and temperature distributions. The building was assumed to have no internal partitions. The effect of the factors affecting on the location of the neutral pressure level (NPL) was of particular interest of the present study.

INTRODUCTION

The air infiltration of a building is mainly due to the characteristics of the wind environment around the structure, the thermal gradient across the building ("thermal effect" or "stack effect"), and the mechanical ventilation.

Since the air infiltration of the building is the direct result of the pressure differences caused by the mechanism mentioned above, it is very important to have correct information on the pressure differentials for the accurate prediction of the air infiltration rate.

The thermal effect in a building is not a negligible factor on the air infiltration during winter, especially where the substantial difference of temperature is observed (Lee, Tanaka and Shaw 1982). Even for one- or two-story houses, the thermal effect in winter is known to be sufficient enough to induce significant air infiltration (Shaw 1979).

For the accurate prediction of the thermal effect, it has been shown that the most important piece of information is to obtain the correct value of the neutral pressure level (NPL), where there is no pressure difference between the inside and the outside of the building (Lee, Tanaka and Shaw 1982).

For the value of NPL, the American Society of Heating, Refrigerating, and Air-Conditioning Engineers (ASHRAE) recommends the following equation (ASHRAE 1981):

$$NPL = \frac{H}{1 + \left(\frac{A_1}{A_2}\right)^2 \left(\frac{T_{in}}{T_{out}}\right)} \quad (1)$$

K.H. Lee, Ph.D. Student, Department of Mechanical Engineering, Y. Lee, Professor of Mechanical Engineering, and H. Tanaka, Associate Professor of Civil Engineering, University of Ottawa, Ottawa, Ontario, CANADA, K1N 6N5.

THIS PREPRINT FOR DISCUSSION PURPOSES ONLY. FOR INCLUSION IN ASHRAE TRANSACTIONS 1985, V. 91, Pt. 2. Not to be reprinted in whole or in part without written permission of the American Society of Heating, Refrigerating and Air-Conditioning Engineers, Inc., 1791 Tullie Circle, NE, Atlanta, GA 30329. Opinions, findings, conclusions, or recommendations expressed in this paper are those of the author(s) and do not necessarily reflect the views of ASHRAE.

Equation 1 is supposed to be applicable only for a simple case with openings at top and bottom levels with no internal partitions between floors, and derived from an assumption that the flow is inviscid.

Consequently, it is reasonable to raise a question if the recommended equation by ASHRAE, Equation 1, can predict the value of NPL accurately for actual buildings. Furthermore, little information has been available until now as to how the various factors, such as the distribution and geometry of the openings, the magnitude of temperature distribution, etc., would affect the thermal behavior of buildings and location of NPL.

In the present investigation, both experimental and analytical studies were made on the characteristics of the thermally induced pressure and on the factors influencing the values of NPL for various cases using an idealized model of a high-rise building with vertically distributed multiopenings and no internal partitions between floors.

ANALYSIS

As is pointed out in the preceding discussion, the accurate prediction of the thermally induced pressure distributions requires the correct value of NPL. In order to obtain the value of NPL, an analytical model shown in Figure 1 is employed. It represents a hypothetical building with n number of openings distributed along elevations and has no internal partitions between floors.

For the present work the following major assumptions are introduced:

1. The inside and outside temperature of the building are constant respectively regardless of elevation;
2. The inside temperature is higher than that of the outside;
3. There exist no wind and mechanical ventilation actions on the buildings; and
4. The flow field at the openings is steady, laminar, and hydrodynamically smooth transition.

From assumptions 1 and 2, the density difference of air between the inside and the outside caused by temperature differences across the exterior wall generates a negative inside pressure differential ($P_{in} < P_{out}$) and induces an inward airflow at the openings below NPL, whereas a positive pressure differential ($P_{in} > P_{out}$) and an outward airflow at the openings exist above NPL. This flow induced by density difference can be analyzed using the energy equation.

From the conservation of energy, the following equation can be formulated at each opening level:

$$\Delta P_k = -\frac{1}{2} [\rho V^2 (1 + \sum K_{f1}) + \overline{CV} \left(\frac{\mu L}{D^2} \right)] \quad \text{Eq. (2)}$$

where $k = i$ or j .

The subscripts i and j refer to the position of the openings existing below and above NPL, respectively. For the case with j , the sign of RHS of Equation 2 becomes negative.

From assumption 4, the friction factor represented in Equation 2 can be given by:

$$f = \frac{C}{Re_d} \quad (3)$$

where

$$\bar{C} = \frac{\int_0^L C dx}{\int_0^L dx}$$

and

$$C_d = 64$$

Using Equation 3 and substituting its corresponding terms into the energy equation, Equation 2, we have

$$\Delta P_{k,i} (P_{out} - P_{in}) = (\Delta P_{k,i} + \Delta P_{f,i} + \Delta P_{fl,i}) \quad (4)$$

For the present model building as shown in Figure 2, Equation 4 becomes as follows:

$$\Delta P_{i} = \frac{1}{2} \left[\rho_a V_a^2 (1+K_c+K_e) + \rho_b V_b^2 (1+K_{re}) + \bar{C}_a V_a \left(\frac{\mu_a L_a}{D_a^2} \right) + \bar{C}_b V_b \left(\frac{\mu_b L_b}{D_b^2} \right) \right] \quad (5)$$

$$\Delta P_{j} = \frac{1}{2} \left[\rho_a V_a^2 (1+K_c+K_e) + \rho_b V_b^2 (1+K_e) + \bar{C}_a V_a \left(\frac{\mu_a L_a}{D_a^2} \right) + \bar{C}_b V_b \left(\frac{\mu_b L_b}{D_b^2} \right) \right] \quad (6)$$

From the mass conservation relationship at the flow field, the continuity equation is given as follows:

$$\sum_{i=1}^M (\rho V A)_i = \sum_{j=1}^N (\rho V A)_j \quad (7)$$

$$(\dot{m})_{in} = (\dot{m})_{out} \quad (8)$$

where M and N are the total number of the openings existing below and above NPL, respectively.

Using the pressure variation in a static fluid and the equation of state for a perfect fluid, the following equation for the stack effect can be obtained:

$$\Delta P_{stack} = K_1 \left(\frac{1}{T_{out}} - \frac{1}{T_{in}} \right) (NPL - Z) \quad (9)$$

Equating Equation 4 with Equation 9; and using the equation of state of ideal fluid, we can now have a general equation to give the value of NPL for the building in which n openings are vertically distributed with no internal partitions between floors as:

$$NPL = \frac{H_j + (X_j/X_i)H_i}{1 + (X_j/X_i)} \quad (10)$$

where

$$X_i = \left[\left(\frac{P_o}{RT} \right) V^2 (1 + \sum K_{f1}) + \left(\frac{\bar{C}_m L}{D^2} \right) V \right]_i$$

$$X_j = \left[\left(\frac{P_o}{RT} \right) V^2 (1 + \sum K_{f1}) + \left(\frac{\bar{C}_m L}{D^2} \right) V \right]_j$$

For the case with openings at top and bottom levels only, Equation 10 reduces to the following expression, Equation 11, because $H_i = 0$, $H_j = H$, $X_i = X_1$, and $X_j = X_2$.

$$NPL = \left[\frac{L}{X_2} \right] H \quad (11)$$

where:

$$X_1 = \left[\left(\frac{P_o}{RT} \right) V^2 (1 + \sum K_{f1}) + \left(\frac{\bar{C}_m L}{D^2} \right) V \right]_1$$

$$X_2 = \left[\left(\frac{P_o}{RT} \right) V^2 (1 + \sum K_{f1}) + \left(\frac{\bar{C}_m L}{D^2} \right) V \right]_2$$

Equation 11 coincides the expression given by ASHRAE, Equation 1, if we disregard the terms associated with the flow frictions in openings.

From overall inspection of Equation 10, it can be seen that the value of NPL has a functional relationship with the variables as follows:

$$NPL = NPL(V, \rho, T, K, f, L, D, A) \quad (12)$$

Since the geometry and temperatures of openings can be determined from given conditions, the solution of Equation 11 would be in terms of flow velocity. In the cases with n numbers of vertical openings, as shown in Figure 1, we will have n set of nonlinear equations in terms of velocity of each openings using the relationships of the mass conservation at openings from Equation 8. These sets of the non-linear equations are solved using a standard computational method available for computers.

EXPERIMENT

Test Section

A plan view of the experimental setup is shown in Figure 2. The system consists of a main test section, pressure, temperature, and power measuring loops, and a data acquisition system.

The main test section, which is designed to simulate the thermal effect in high-rise buildings, is made of a copper tube with 50.8 mm I.D. and 18.3 m in length. In order to achieve any given temperature distribution inside the test section along elevations, the test section is fabricated with 20 individual heating units. Each heating unit is 0.91 m in length and its heating power supply is controlled independently by its own variable transformer.

One K-type (chromel-alumel) thermocouple was spot-welded on the outer surface of each individual heating unit at the center. The outer wall of the copper tube was then coated with thermal resistant electric insulation paint and wrapped with three layers of 50 mm wide fiberglass tapes. Seventeen-gauge nichrome wires were wound around the pipe in 40 mm pitches over the length of 0.91 m to construct a heating unit. To simulate the effect of distributed cracks and openings in buildings, six openings are provided on the wall of the test section along elevations, as shown in Figure 2.

For the measurement of air temperature inside the test section, five sets of 20.0 mm long, seventeen-gauge hypodermic stainless steel tubing were mounted through the wall for the insertion of thermocouples.

Pressure taps made of seventeen-gauge hypodermic stainless steel tubing of 76.2 mm long were mounted also through the test section wall at seven elevations, as shown in Figure 2.

The entire test section was then covered with 40 mm thick glassfibre insulation.

Instrumentation and Data Acquisition System

Pressure Measurements: The measurement of the pressure difference across the exterior wall of the test section was made with seven sets of pressure transducers with maximum pressure head of 1 torr (133 Pa) and 0.15% error at full scale.

One of two pressure ports of each transducer was connected to the pressure tap of the test section and another port was connected to a 17-gauge stainless steel tube mounted immediately outside the test section at the same elevations.

The signals from pressure transducers are sent to the data acquisition system.

Temperature Measurements: Thirty eight K-type thermocouples are used in total for the measurement of temperature profiles of the test section. Twenty thermocouples are spot-welded on the outer surface of the copper tube of the test section (at the center of each heating unit) to measure the wall temperatures of the test section. In addition, eight thermocouples were provided on the outside surface of the test section to supplement the 20 thermocouples mentioned above. Five thermocouples which are sheathed K-type 152 mm long, 0.82 mm O.D stainless steel tubing are inserted into the temperature measuring tap of the test section to measure the inside air temperature along the elevation. Another five were placed outside to measure the variation of the outside temperature along the test section.

Control and Measurement of Power: Twenty sets of variable transformers with 1 KW capacity, 110 V and 10 A are used to supply and control the power to each heating unit. The power is measured by both a digital voltmeter and amperemeter through the measuring circuits. The measured data of power supplied are manually entered into the data acquisition system.

Data Acquisition System: The data acquisition system used in the present study consists of a desk top computer with a digital voltmeter, a scanner, a printer/plotter and a real time clock. The raw and reduced data are stored in magnet tapes; hard copies were also made available.

Experimental Procedures

Preliminary: The following preliminary steps are taken prior to the actual experiment for a given test condition: (1) the electric insulations of all wirings of heating units, the connections of all thermocouples employed, and pressure transducers are checked; (2) the zero adjustment of all pressure transducers is made; and (3) the power supply and control system are switched on and idled for more than 12 hours to attain the stable temperature distribution in the test section.

Simulation of Thermal Effect: The simulation of thermal effect is carried out through careful and cautious adjustment of power supply to each heating unit with continuous measurements of current and voltages supplied and the temperature distribution along the test section. This procedure is continued until the desired temperature distribution is achieved with the maximum allowable wall temperature deviation of 3°C at each point. The range of temperature difference across the wall of test section in this study is between 25 and 60°C (25, 30, 40, 50, and 60).

RESULTS AND DISCUSSIONS

Validity of Stack Effect Equation

As stated earlier, Equation 9, the stack effect equation, which was derived from the equation of static fluid and state of perfect gas, can be used to predict correctly the pressure differentials induced by thermal effect, if the correct value of NPL is provided.

To evaluate the validity of Equation 9, the coefficient K_{st} of the stack effect equation is calculated using the experimental data obtained for various values of temperature differences and opening conditions. The results plotted in Figure 3 illustrate that the value of K_{st} obtained from experimental data is found to be in excellent agreement with the theoretical value. The experimental observation is shown to be approximately 3.5×10^3 Pa.K/m, and this also confirms the findings of Lee, Tanaka and Shaw (1982). From this result, we may conclude that the stack effect equation, Equation 9, can be used with great confidence to predict pressure differentials induced by thermal effect if the value of NPL is known correctly.

Comparison of Test Results with Analysis

Figure 4 is an illustration of the comparison between the predicted and measured values of NPL for the cases with openings at top and bottom level only. The predicted value of NPL is obtained from Equation 11. The values of the NPL calculated with the correlation recommended by ASHRAE, Equation 12, are also plotted and compared in Figure 4.

Figure 5 shows a typical comparison between the predicted values of NPL and the experimental results, and the ASHRAE correlation for the cases with

openings at top and bottom level only. As illustrated in Figure 4, the results obtained using ASHRAE recommendation exhibit a considerable discrepancy from the experimental results. However, the predicted value of NPL based on Equation 11 demonstrates an excellent agreement with the measured results. While the deviation of the ASHRAE recommendation is found to be up to 25%, the results obtained from the present analysis show less than 6% deviation from the experimental results in all cases studied, as shown in Figures 4 and 5.

The Figure 6 represents a comparison of the predicted values of NPL obtained from Equation 10 to the results obtained from the experiments for the cases with three or four vertically distributed openings. The agreement between the value of NPL predicted by the present analysis and that obtained from the experiment is excellent.

Since Equation 1, recommended by ASHRAE, is for openings at two levels only, it was not possible to compare it with the present results.

From an overall examination of the results discussed above, it is found that the analytical model for the prediction of NPL must consider the actual flow conditions closely, including flow channel geometry. The significant disagreement between the results obtained from the ASHRAE recommendation and the present study may be attributed to the fact that Equation 1 is derived for inviscid flow, thus neglecting the effect of flow resistances along the flow path.

The ASHRAE recommendation overly simplifies the factors that must be considered in actual situations and cannot be an accurate method for the predicting the value of NPL in reality. It leads to a conclusion that the effect of flow resistance on the value of NPL is not negligible and should be taken into the consideration for the accurate prediction of the value of NPL, hence for the prediction of the pressure differential induced by the thermal effect.

Effect of Opening Distributions

A series of tests was performed to investigate the influence and sensitivity of the vertical distribution of openings on the value of NPL. Figure 7 illustrates one of the test results obtained in the experiment for various opening modes while the temperature difference across the test section wall was kept constant.

Figure 7 reveals clearly that the effect of the opening conditions on the value of NPL strongly depends on the opening mode imposed. Test Numbers 1 and 12 in Figure 7 represent the profile of pressure differentials for the cases with openings at top or bottom level only, respectively. This coincides with the results that can be predicted from Equation 10 and demonstrates the accuracy of the experiments executed.

The same trends were observed in all other tests.

Effect of Temperature Difference

Equation 9 expresses that the pressure differentials induced by thermal effect are proportional to the difference of the reciprocal of the inside and the outside absolute temperature for a given value of NPL.

In order to study the effect of temperature differences on the value of NPL, a series of experiments was conducted for various temperature differences, while the opening condition was kept constant. A typical set of these test results is shown in Figure 8. From the figure, it can be seen that the pressure differentials induced by thermal effect are proportional to the difference of the reciprocal of the inside and the outside absolute temperature as expected from Equation 9, but the value of NPL is hardly influenced by temperature differences for the given opening conditions.

In all other tests, in which the opening condition was kept constant but temperature differences imposed were varied, the same trends were observed as in Figure 8. This trend can be also supported by the result of the field test conducted by Tamura and Wilson (1966) in a commercial building.

From the above observation, we may conclude that the absolute magnitude of temperature difference (within a realistic range) across the exterior wall of building does not have significant effect on the value of NPL, but the thermal effect is mainly decided by the difference of the reciprocal of the inside and the outside absolute temperatures for a given opening mode.

Effect of Physical Dimensions

As has been demonstrated above, Equation 10 derived from the consideration of the actual flow conditions associated with openings, shows an excellent agreements with the measured test results in all the cases studied. It is therefore possible to evaluate the effect of the physical dimensions of buildings on the value of NPL from Equation 10. Only the case with openings at top and bottom levels was considered here.

In the analysis, the length and the inside diameter of the test section used in the experimental program, 18.3 m and 50.8 mm, are used as the reference dimensions of L_0 and D_0 , respectively.

Figure 9 illustrates the effect of the vertical dimensions of buildings on NPL, where the elevation of NPL is plotted as a function of the dimensionless building height, (L/L_0) . The value of NPL seems to be constant for the cases of opening conditions studied when the value of the ratio, (L/L_0) , is greater than about 0.5.

Figure 10 shows the effect of the lateral dimension of buildings on the value of NPL, where the ratio of the lateral dimensions of buildings, (D/D_0) , is plotted against the dimensionless height for a given condition. It can be seen that the effect of the ratio, (D/D_0) , on the value of NPL is insignificant when the value of the ratio, (D/D_0) , is greater than about 0.4.

It may be concluded from Figures 9 and 10 that the effect of the physical dimensions of buildings on the value of NPL is negligible when the values of the ratios (L/L_0) and (D/D_0) are greater than about 0.5 and 0.4, respectively.

CONCLUSIONS

Based on the present analysis and experiment, the following conclusions may be drawn:

1. The stack effect equation, derived from equation of static fluid and state of ideal gas, is applicable for the prediction of the pressure differentials induced by the thermal effect, provided the value of NPL is known correctly.
2. The pressure differentials caused by the thermal effect is shown to be linearly proportional to the difference of the reciprocal of the absolute temperature of the inside and the outside of buildings.
3. The effect of flow resistance in the flow paths of the openings on the value of NPL is appreciable, and its effect should be taken into consideration for the accurate prediction of the thermal effect.
4. The value of NPL is significantly influenced by the distributions of the openings in buildings.

5. The effect of the difference between the inside and outside temperature of buildings on the value of NPL is negligibly small for a given distribution of the cracks and openings, within a practical range of temperature variation.
6. The effect of the physical dimensions of buildings on the value of NPL is shown to be insignificant where the dimensionless parameters, (L/L_0) and (D/D_0) , are greater than about 0.5 and 0.4, respectively, for the case studied.
7. The existing method recommended by ASHRAE to predict the value of NPL is shown to be inadequate for the accurate prediction of NPL in actual situations in reality.

NOMENCLATURE

- A = area of openings
- C = coefficient in Equation 3
- D = diameter of openings
- f = friction factor
- g = acceleration of gravity
- H = height of building from bottom opening
- K = the form loss factor
- K_1 = constant in Equation 9
- L = the length of flow path
- n = total number of openings
- NPL = the elevation of neutral pressure level from bottom opening
- P = pressure
- P_0 = the standard atmospheric pressure
- R = gas constant of air
- Re = Reynolds number at openings
- T = temperature
- V = flow velocity
- Z = elevation of opening from ground

Subscripts

- a = flow section a of openings (Figure 2)
- b = flow section b of openings (Figure 2)
- c = sudden contraction of flow area
- d = fully developed

e = sudden expansion of flow area
f = friction; friction factor
fl = form loss
i = position of openings below NPL
in = inside
j = position of openings above NPL
K.E. = kinetic energy
out = outside
re = reentry section of flow area
x = local; developing
1 = top level
2 = bottom level

Greek Symbols

μ = dynamic viscosity
 ρ = fluid density

REFERENCES

- ASHRAE. 1981. ASHRAE handbook--1981 fundamentals. Chap. 22. Atlanta: American Society of Heating, Refrigerating, and Air-Conditioning Engineers Inc.
- Lee, Y., Tanaka, M. and Shaw, C.Y. 1982. "Distribution of wind and temperature induced pressure differences across the walls of a twenty story compartmentalized building." Journal of Wind Engineering and Industrial Aerodynamics, Vol. 10, 287-301.
- Shaw, C.Y. 1979. "Air Tightness and Air Infiltration of School Buildings", ASHRAE Transactions, Vol. 85, 85-95.
- Tamura, G.T. and Wilson, A.G. 1966. "Pressure Differences for a Nine Story Building as a Result of Chimney Effect and Ventilation System Operation", ASHRAE Transactions, Vol. 72, Part.I, p. 180.

ACKNOWLEDGMENT

The present study is financed by the Natural Science and Engineering Research Council of Canada, under the strategic grant (energy).

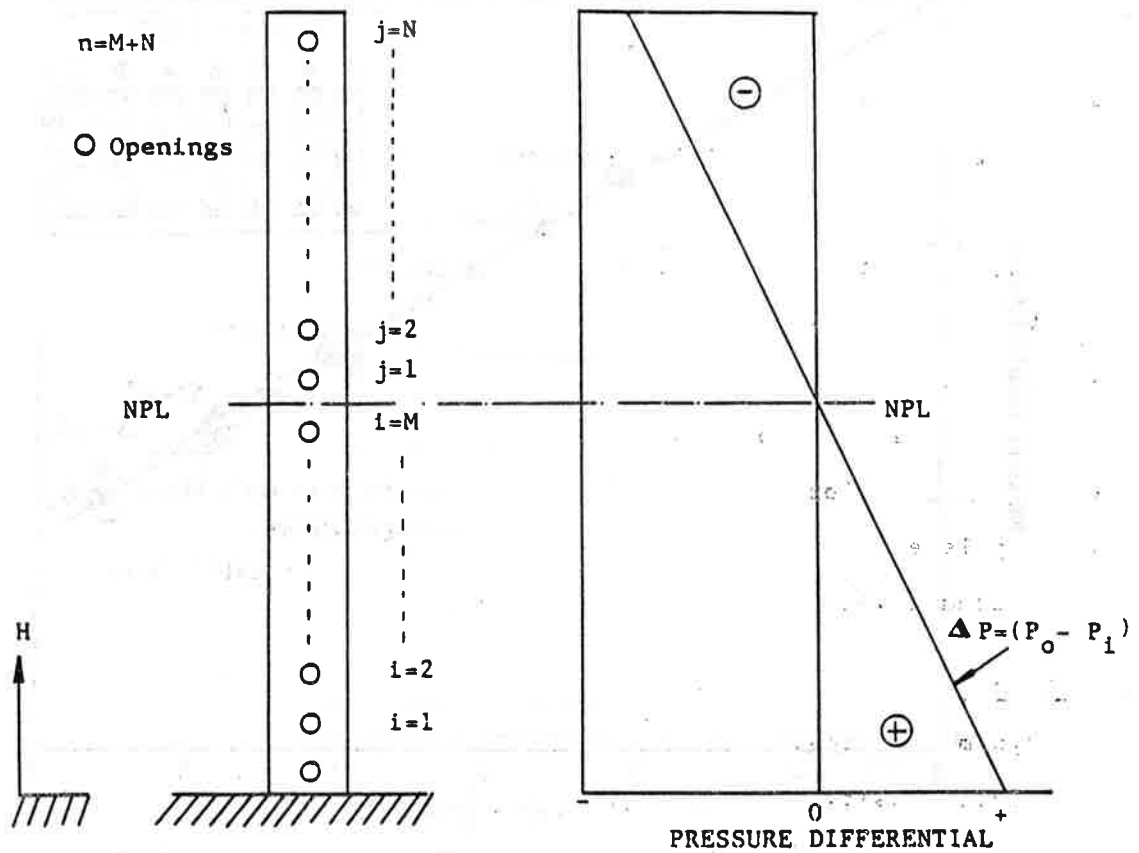


Figure 1. Idealized model building and thermal effect

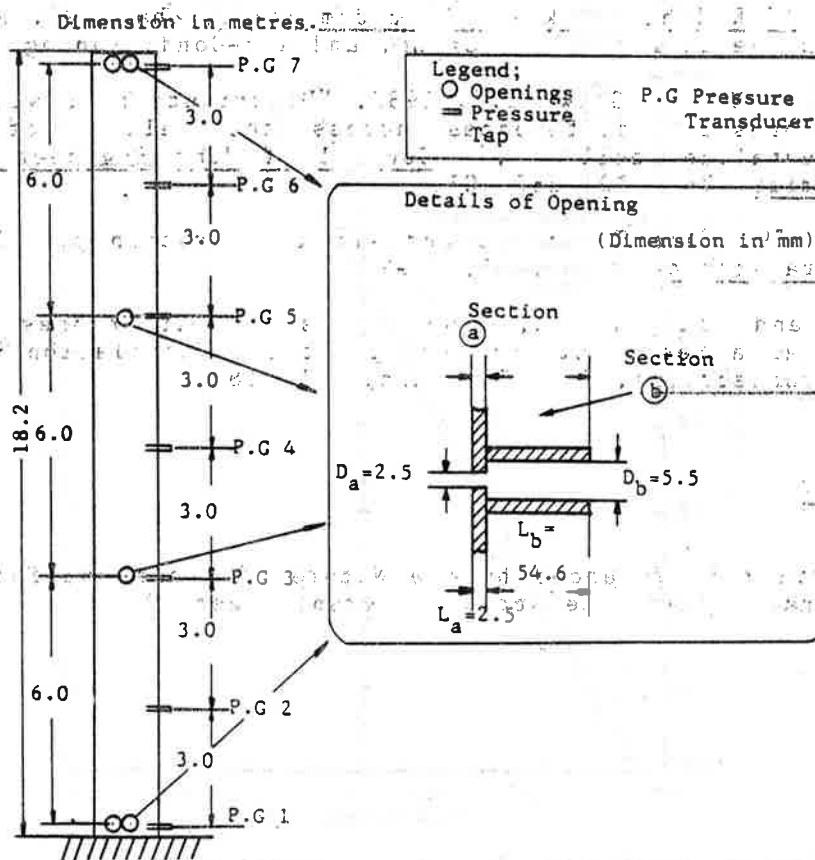


Figure 2. The details of openings

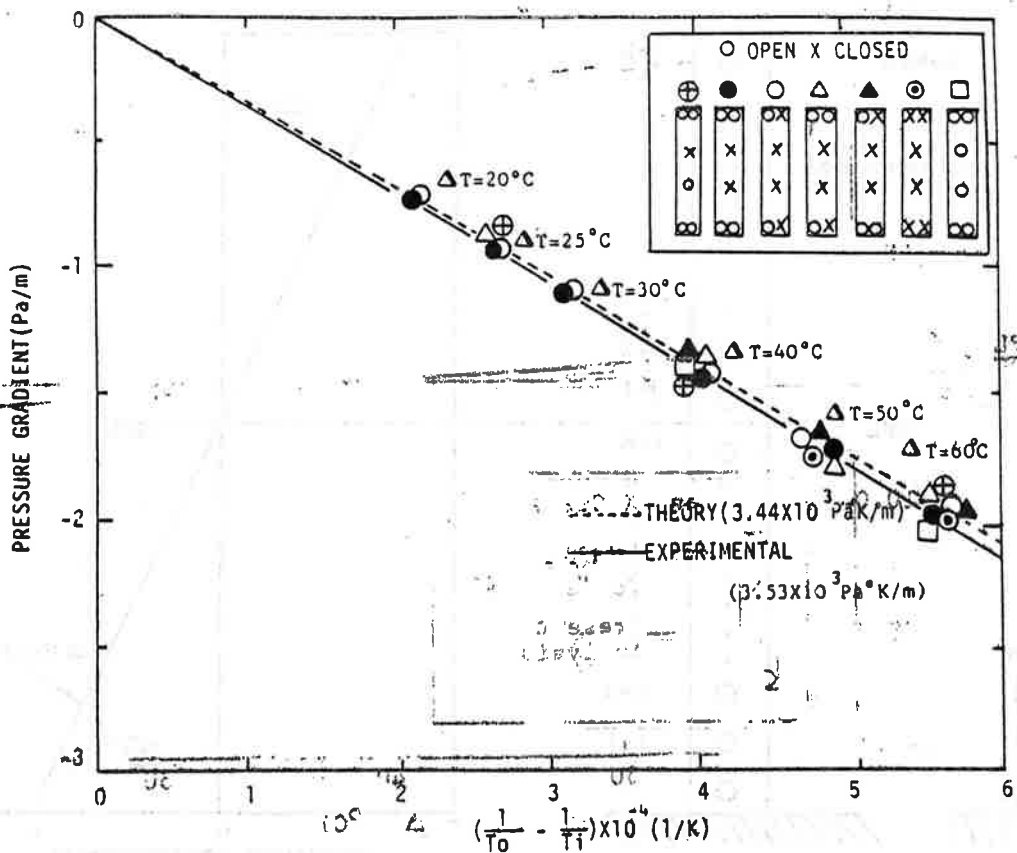


Figure 3. Vertical pressure gradient due to thermal effect

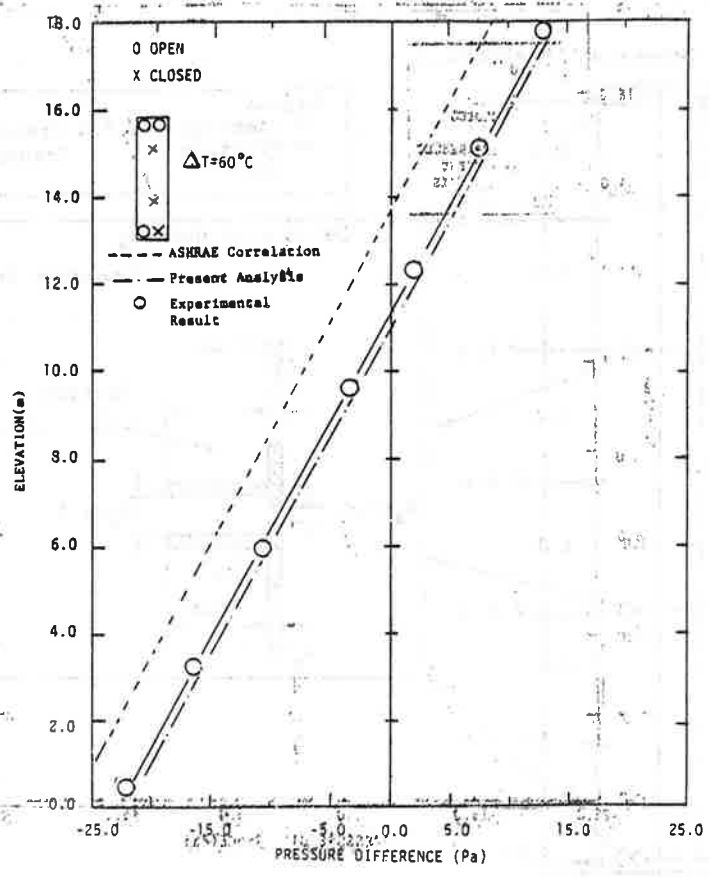


Figure 4. Comparison of experimental results with ASHRAE recommendation and present analysis

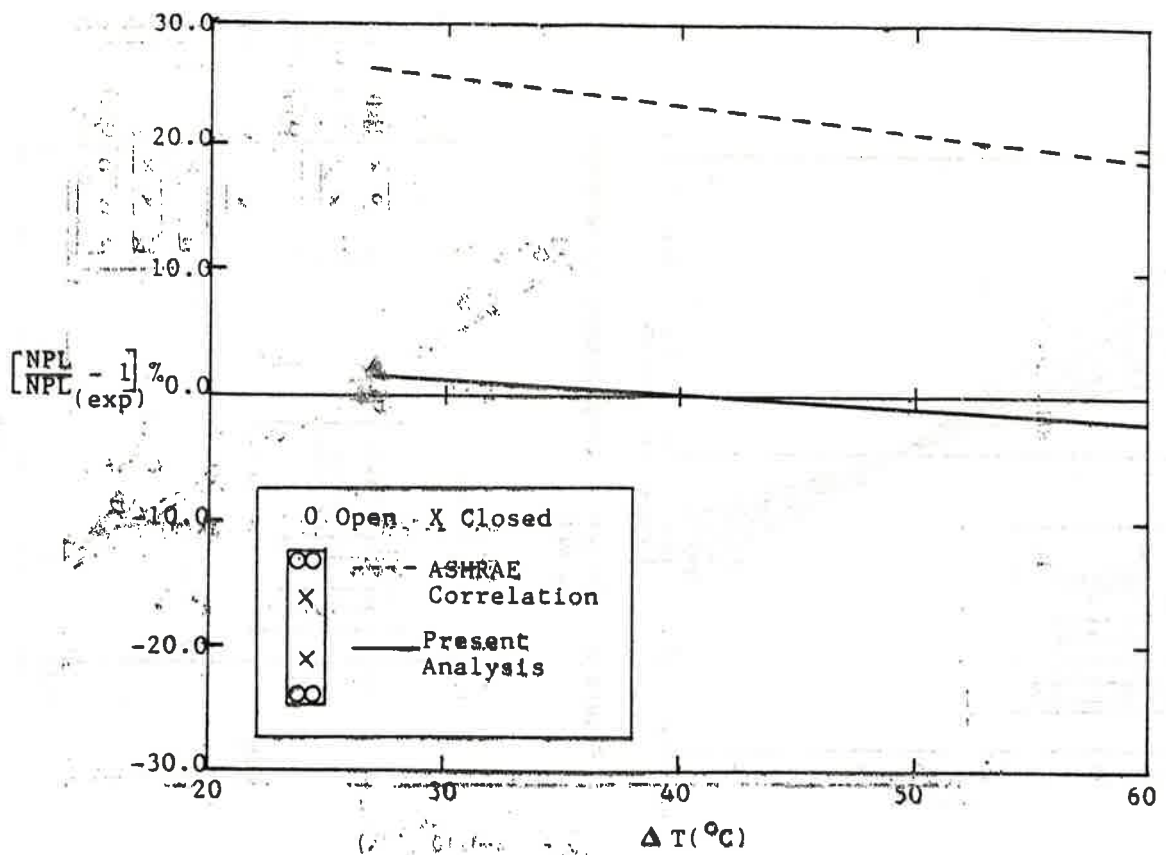


Figure 5. Comparison of experimental results with ASHRAE recommendation and present analysis with experimental results

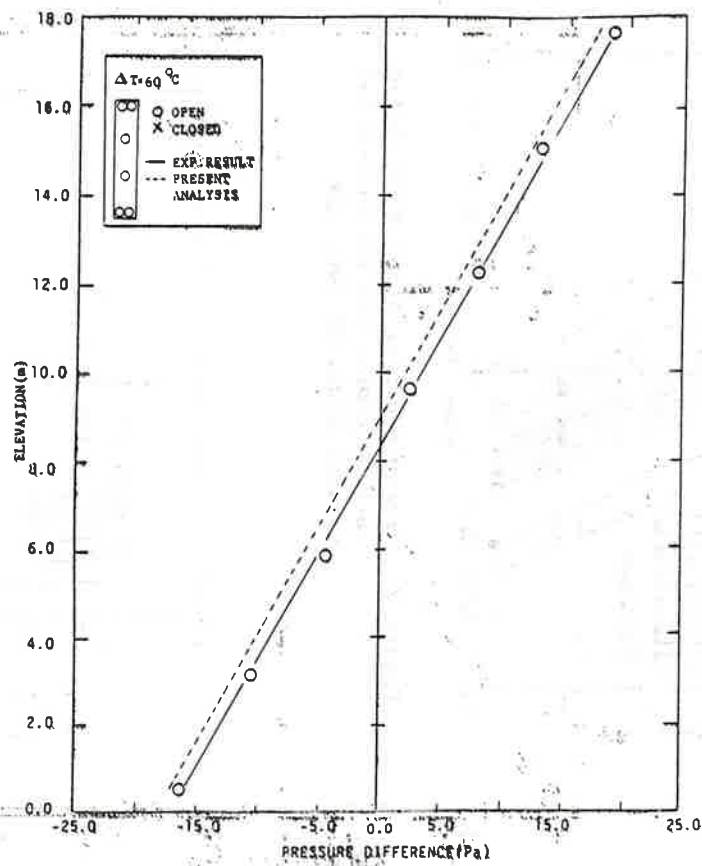


Figure 6. Comparison of experimental results with analysis multi-openings

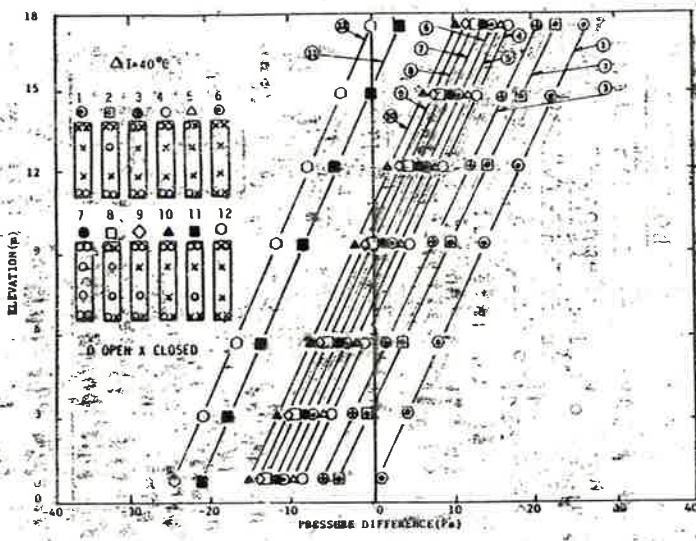


Figure 7. Pressure differential distribution versus temperature difference for various modes of openings

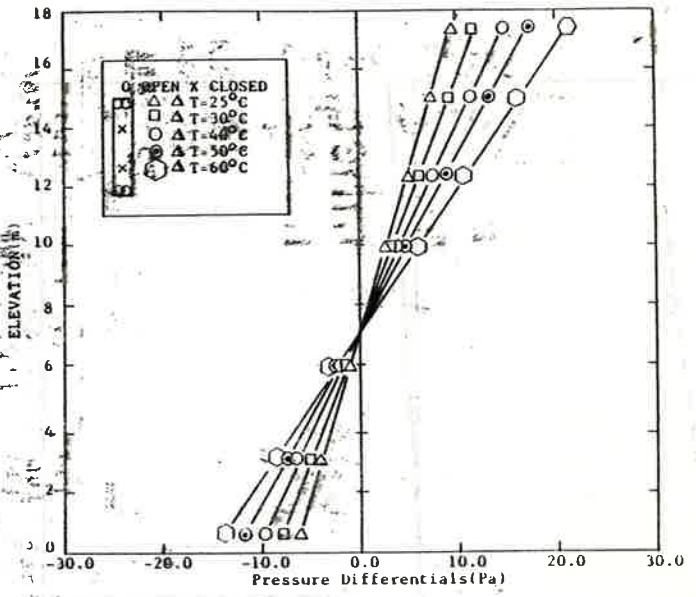


Figure 8. Effect of temperature difference on NPL

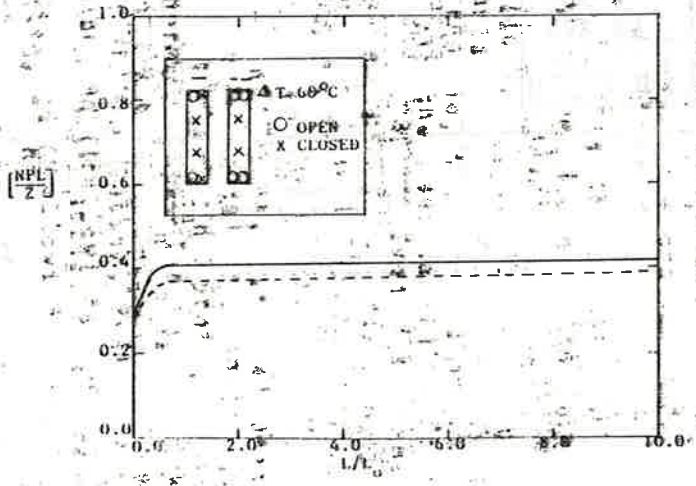


Figure 9. Effect of vertical dimension of building on NPL

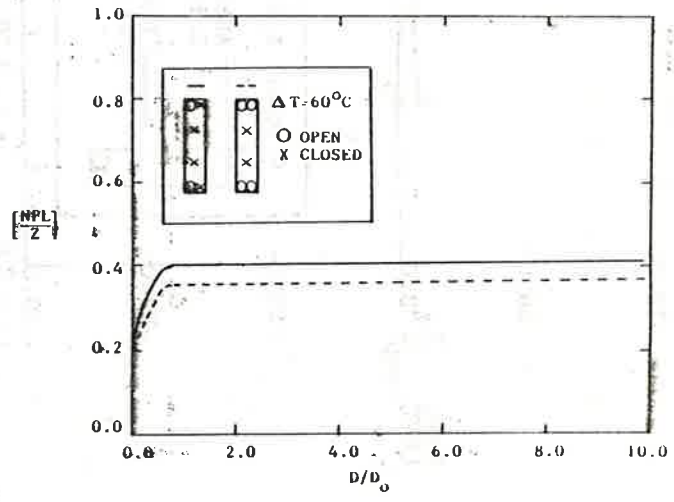


Figure 10. Effect of lateral dimensions of building on NPL